All-fullerene Electron Donor-Acceptor Conjugates

Marta Izquierdo,[a]+ Benedikt Platzer,[b]+ Antony J. Stasyuk,[c] Olga A. Stasyuk,[c,d] Alexander A. Voityuk,[c,e] Sergio Cuesta,[a] Miquel Solà,[c]* Dirk M. Guldi,[b]* and Nazario Martín[a]*

Dedicated to Prof. Jean-Marie Lehn on the occasion of his 80th birthday

Abstract: *The synthesis and characterization of a covalent all-fullerene* ***C_{60}-$Lu_3N@I_h$-C_{80}*** *electron donor-acceptor conjugate has been realized by sequential 1,3-dipolar cycloaddition reactions of azomethine ylides on $Lu_3N@I_h$-C_{80} and C_{60}. To the best of our knowledge, this is the first time that two fullerenes behaving as both electron donor ($Lu_3N@I_h$-C_{80}) and acceptor (C_{60}) are forming an electroactive dumbbell. DFT calculations reveal up to 16 diastereomeric pairs, that is, 8 syn and 8 with anti orientation, being the anti-RSSS isomer the most stable. Spectroelectrochemical absorption and femtosecond transient absorption experiments support the notion that a $C_{60}^{\bullet-}$-$Lu_3N@I_h$-$C_{80}^{\bullet+}$ charge-separated state is formed. Spin conversion of the singlet $C_{60}^{\bullet-}$-$Lu_3N@I_h$-$C_{80}^{\bullet+}$ charge-separated state into the triplet $C_{60}^{\bullet-}$-$Lu_3N@I_h$-$C_{80}^{\bullet+}$ charge-separated state is facilitated by the heavy atom affect stemming from the Lu_3N-cluster and, in turn, slows down the charge recombination by one order of magnitude.*

Converting light into chemical energy by means of photoinduced electron transfer (ET) is key to natural photosynthesis of plants and bacteria. In the reaction centers, a cascade of charge separation and charge shift reactions yields long-lived charge-separated states in nearly quantitative quantum yields.[1][2] A broad variety of artificial photosynthetic systems based on multi-component electron donor-acceptor conjugates have enabled mimicking those steps seen in natural photosynthesis.[3] To this end, C_{60} stands out as a redox active component.[4] To a much lower extend, endohedral fullerenes – which encapsulate atoms, molecules, ions, or clusters – have been integrated into electron donor–acceptor systems. Interesting is the fact that they stabilize charge-separated states when compared to C_{60}.[5]

Notably, empty fullerenes, in general, and C_{60} in particular, turned into electron acceptors of choice. In contrast, some endohedral fullerenes exhibit remarkable electron donating features: In the presence of strong electron acceptors such as tetracyano-*p*-quinodimethanes (TCNQ)[6] or perylene bisdiimides (PDI),[7] charge-separated states are formed, in which the endohedral fullerene are one-electron oxidized.

The trimetallic nitride template (TNT) family with the general formula $M_3N@C_{2n}$ is more stable than any other endohedral metallofullerenes (EMF). In particular, $Lu_3N@C_{80}$ is one of the best-studied endohedral metallofullerenes. Considering a much lower oxidation when compared to C_{60}, renders TNTs a much better choice as electron-donor in electron donor-acceptor conjugates.[8]

As far as electron transfer reactions are concerned, TNTs have been shown to provide the ways and means to spin convert charge separated states. To this end, the stabilization of a triplet charge separated state relative to a singlet charge separated state is quite significant. But, it is not solely the difference in spin, which is decisive, the energy difference, which is due to the exchange interaction, is another important factor for slowing down the charge recombination. Formation of a triplet charge separated state was recently shown for the case of TNT, when linked covalently to a PDI. Remarkable was the stabilization when contrasted with the singlet charge separated state: an impressive factor of nearly 1000 evolved. Notable is, however, that electron accepting PDIs reveal rather large reorganization energies in electron transfer reactions. Quite different is the scenario for C_{60}:[9],[10] What stands out among the many unique features of C_{60} is it small reorganization energy in electron transfer reactions. The consequences of the small reorganization energy are far reaching: For example, charge recombination, as the most critical parameter to impact photocatalysis and photovoltaics, is pushed into the Marcus inverted region and, in turn, slowed down.

In light of the aforementioned, integrating, for example, $Lu_3N@I_h$-C_{80} as electron donor together with C_{60} as electron acceptor into an electron donor-acceptor conjugate is the way to go en-route towards long-lived charge separation. This is, where the current work makes a significant contribution; we have designed, synthesized, and probed a C_{60}-$Lu_3N@I_h$-C_{80} dumbbell and have demonstrated that the triplet charge

[a] Dr. M. Izquierdo, Mr. S. Cuesta, Prof. Dr. N. Martín
Departamento de Química Orgánica, Facultad de Ciencias Químicas, Universidad Complutense, 28040 Madrid, Spain.
E-mail: nazmar@ucm.es
[b] Mr. Benedikt Platzer, Prof. Dr. Dirk M. Guldi
Department of Chemistry and Pharmacy
Friederich-Alexander Univesität Erlangen-Nürnberg
Nikolaus-Fiebiger-Str. 10
E-mail: dirk.guldi@fau.de
[c] Dr. A. J. Stasyuk, Dr. O. A. Stasyuk, Prof. Dr. A. A. Voityuk, Prof. Dr. M. Solà, miquel.sola@udg.edu
Institute of Computational Chemistry and Catalysis and Department of Chemistry
University of Girona
C/ M. Aurèlia Capmany, 69, 17003 Girona, Spain.
[d] Dr. O. A. Stasyuk
Institute of Organic Chemistry and Biochemistry
Academy of Sciences of Czech Republic
Flemingo nám. 2, 166 10 Prague, Czech Republic.
[e] Institució Catalana de Recerca i Estudis Avancats (ICREA), 08010 Barcelona, Spain.
+ These authors contributed equally to the work.

Supporting information for this article is given via a link at the end of the document.

separated state is longer-lived by nearly two orders of magnitude when compared to the corresponding singlet charge separated state. Our work has been rounded off by DFT calculations at the BLYP-D3(BJ)/def2-SVP level of theory to shed light onto relative thermodynamic stability of the 16 possible stereoisomers!

Synthesis of *all-fullerene* 6a/6b. It is well known that the reactivity of TNTs is different from that of empty fullerenes; therefore, it requires a specific strategy. The retrosynthetic analysis of the *all-fullerene* dumbbell, in which C_{60} and $Lu_3N@I_h$-C_{80} are linked via a phenyl linker indicates two possible synthetic routes – Scheme 1.

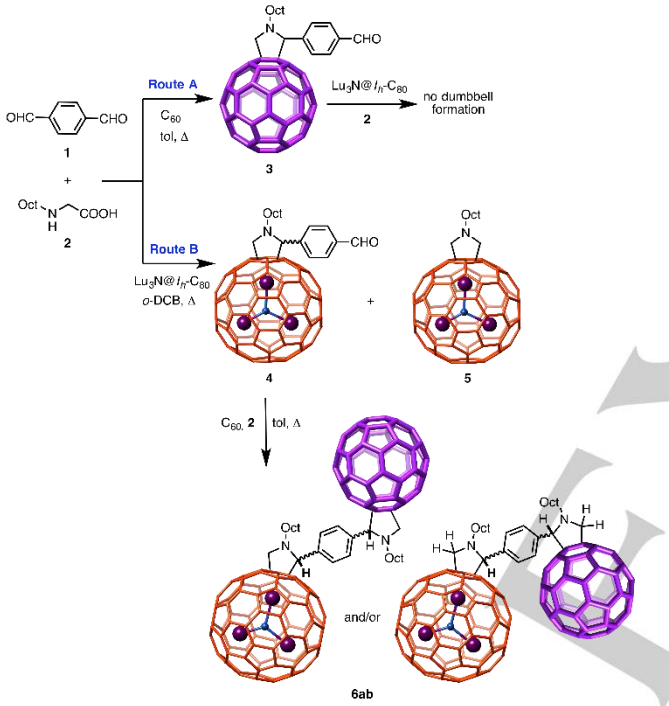

Scheme 1. Synthesis of **6a/6b** from 1,3-dipolar cycloaddition reaction (see theoretical calculations).

In route A, the reaction of terephthalaldehyde **1** and *N*-octylglycine **2** with C_{60} afforded exclusively aldehyde **3**. The 1,3-dipolar cycloaddition reaction with $Lu_3N@I_h$-C_{80} was, however, unsatisfactory. The lack of dumbbell formation is rationalized by the lower reactivity of $Lu_3N@I_h$-C_{80} relative to C_{60}. Route B yielded the desired **6a/6b** from aldehyde **4**. Formation of aldehyde **4** also afforded side-product **5**, which lacked the *p*-formylphenyl group. **5** was formed by the addition of the *N*-octylglycine to the fullerene in competition to the 1,3-dipolar cycloaddition, presumably through an electron transfer/radical mechanism. Similar reactions have been reported for C_{60} and $Gd@C_{82}$.[11] When monoadduct **4** was refluxed in toluene in the presence of C_{60} and *N*-octylglycine, **6a/6b** were obtained as main products. The structure of **6a/6b** was confirmed by mass spectrometry showing molecular peaks at m/z= 2605.039 uma. Both of them were isolated by HPLC and characterized by a variety of spectroscopic techniques (SI).

To predict the structure of **6a/6b** we considered the following: First, cycloaddition to $Lu_3N@I_h$-C_{80} takes place on a [5,6]-bond affording the thermodynamic product.[12] Second, **6a/6b** possess four chiral centers, that is, two at the nitrogen atoms and two at the C2 of the pyrrolidine rings, and, in turn, a total of 16 stereoisomers are possible. Third, depending on the relative orientation of C_{60} and $Lu_3N@I_h$-C_{80} with respect to the plane of the phenyl linker, **6a/6b** might be a *syn*- or an *anti*-isomer. As such, 32 is the maximum theoretical number of isomers. However, since enantiomeric pairs are physically and chemically indistinguishable, only 16 stereoisomers, namely 8 of them corresponding to *syn* and 8 corresponding to *anti* orientation, were considered in the present theoretical study (see Figure 1 for *syn* and *anti* RSSS).

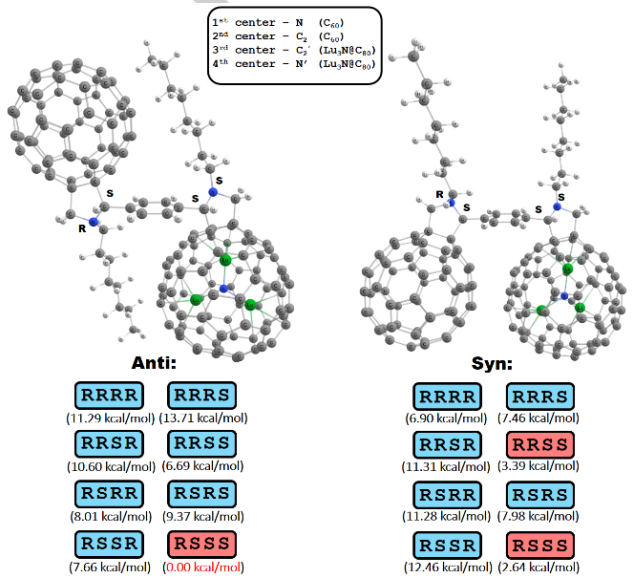

Figure 1. Structures of the *anti* RSSS and *syn* RSSS stereoisomers of **6a/6b**. CAM-B3LYP-D3(BJ)/def2-SVP//BLYP-D3(BJ)/def2-SVP relative energies for all 16 isomers. The three most stable isomers (within 5 kcal/mol) are marked with red.

Stability of *all-fullerene* 6a/6b stereoisomers. DFT and TDA-DFT calculations at the CAM-B3LYP-D3(BJ)/def2-SVP//BLYP-D3(BJ)/def2-SVP level of theory (see SI for complete computational details) revealed that all isomers are in the energetic range of 14 kcal/mol – Figure 1. The most stable isomer is *anti*-RSSS. Two *syn*-isomers, that is, *syn*-RRSS and *syn*-RSSS, lie in the range of 5 kcal/mol. In order to understand the relative stability QTAIM calculations for the most stable structures have been performed.[13]

To characterize the excited states, each isomer was divided into 6 fragments – Figure S16: (1) Lu_3N; (2) I_h-C_{80} + pyrrolidine; (3) C_{60} + pyrrolidine; (4) C8 chains attached to I_h-C_{80} (5) and C8 chains attached to C_{60}; (6) phenyl linker. Next, exciton delocalization and charge transfer contributions in each fragment were analyzed for the lowest 80 excited states of each

isomer. Locally excited states (LE), where the exciton is mostly localized on a single fragment (charge separation value < 0.1e), charge separated (CS) states, where the electron density is redistributed between fragments (charge separation > 0.9e), as well as mixed states (CT states) with partial charge transfer (charge separation between 0.1e and 0.9e), where significant LE and CS contributions are present, were identified.

Excited state calculations were performed for the three isomers of lowest energy: *syn*-RRSS and *syn*-RSSS as well as *anti*-RSSS. In the gas phase, the energies of the predicted singlet excited states range from 2.0 to 3.8 eV –Table S2. For each isomer, the LE states on $Lu_3N@I_h$-C_{80} have the lowest energy. They are best described as HOMO-to-LUMO+2 transitions. LE states on C_{60} are 0.22-0.32 eV higher and correspond to HOMO-4-to-LUMO transitions. The first CS/CT states (CS1/CT1) are found at around 3.0 eV for all three isomers – Table S2. In the case of *syn*-RRSS and *syn*-RSSS, the charge transferred from $Lu_3N@I_h$-C_{80} to C_{60} is about 0.5 – 0.6 e^- (CT states), while almost 1 e^- is transferred in *anti*-RSSS (CS states). In the gas-phase, $Lu_3N@I_h$-C_{80}-to-C_{60} CS/CT states have relatively small probabilities with oscillator strengths that are in the range from 0.001 to 0.02. Notably, similarly low oscillator strengths were associated with the lowest LE states. Molecular orbitals representing both LE, CS, and CT states shown in Figure S17.

Solvent effects for *all-fullerene* 6a/6b. A COSMO-like model was applied with dichloromethane (DCM) as solvent. Solvation energies for the *syn*- and *anti*-isomers are around 0.24 eV for their ground states (GS) and they exert no notable effects on the relative energies of the LE states relative to the ground states. By virtue of similar dipole moments for the GS and LE states, the energies of the LE excitations remain almost unchanged.

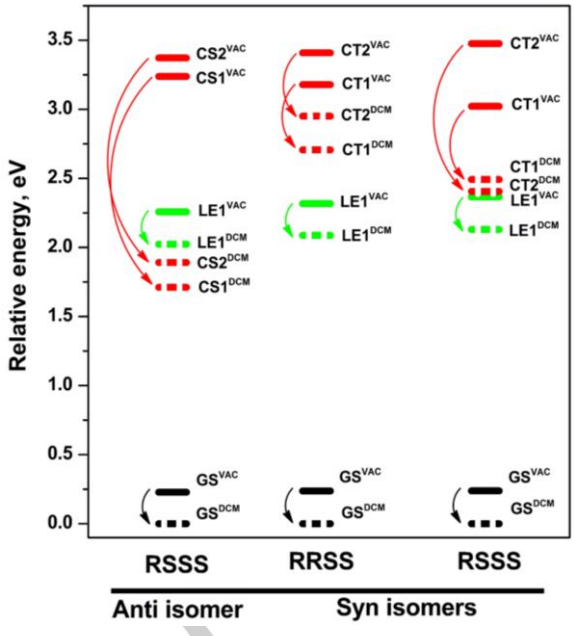

Figure 2. Relative energies in eV of the ground states (GS), the first LE state, (LE1), and the CS/CT states (CS1/CT1, CS2/CT2), in the *anti*-RSSS, *syn*-RRSS, and *syn*-RSSS computed in vacuum (VAC) and dichloromethane (DCM). CS1/CT1 and CS2/CT2 are due $C_{80} \rightarrow C_{60}$.

As expected, the dipole moments of the CS/CT states differ significantly from those of the LE and GS states – Table S3. For the lowest CS/CT states in *syn*-RRSS, *syn*-RSSS, and *anti*-RSSS, the dipole moments are calculated to be 23, 25, and 63 D, respectively. The differences in dipole moment of the *syn*- and *anti*-stereoisomers are rationalized by a larger electron donor-acceptor distance in anti-RSSS of 14 Å, as compared to syn-RRSS and syn-RSSS of 10 Å. Also, charge transfer for *syn*-RRSS and *syn*-RSSS involve about 0.5 – 0.6 e^-, whereas for *anti*-RSSS it is equivalent to 1 e^-. Figure 2 displays the GS, LE, and CS/CT energies for the singlet excited states in the gas phase and in DCM. As seen, the population generation of CS1 and CS2 through charge separation of LE1 state is possible only for the *anti* RSSS isomer in DCM (CS states have lower energies than LE1 state).

Electron transfer rates in *all-fullerene* 6a/6b. The non-adiabatic ET rates, k_{ET}, were estimated using the classical Marcus equation[14] (for details see SI). To this end, three key ET parameters were computed: free energy ΔG, electronic coupling V and, reorganization energy including both the internal and solvent terms (for fragment definition see Figure S18). Using the computed data, which is listed in Table 1, we estimated the rates for charge separation and charge recombination

Table 1. Electron transfer parameters and rates for charge separation reactions in DCM calculated for *anti*-RSSS.

Type	ΔG_0, eV	|V|	Reorganization energy λ, eV	Rate constant, s^{-1}
LE1→CS1	-0.313	0.0041	0.828	$1.361 \cdot 10^{10}$
LE1→CS2	-0.133	0.0183	0.813	$2.464 \cdot 10^{10}$

Charge separation, LE1 → CS1 and LE1 → CS2, is fast with k_{CS} ≈ 13 and 24 ns^{-1}, respectively. Note that the corresponding charge recombination reactions are in the inverted Marcus region and cannot accurately be estimated. Figure 3 highlights the electron transfer processes following photoexcitation of the *anti*-RSSS and the *syn*-RRSS isomers. Analysis of excited states revealed that the singlet and triplet CS states have similar energies, which facilitate intersystem crossing between them.

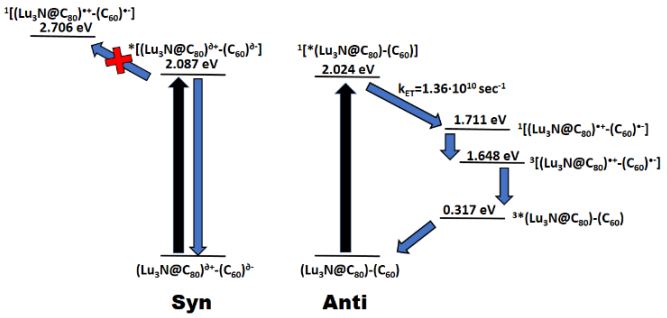

Figure 3. Summary of the computational results for the first LE and CS of singlet and triplet states for the anti-RSSS and the syn-RRSS computed in DCM.

Ground-state characterization of *all-fullerene* 6a/6b[15] The absorption spectrum of **6a/6b** (Figure S19) reveals, on one hand, the same features as those seen for C_{60}, namely a maximum at 432 nm, which evolves as a well-known marker for the successful functionalization of C_{60}, followed by a weaker maximum at around 700 nm.[16] On the other hand, a rather broad maximum is observed for **6a/6b** at about 860 nm, similar to that of 850 nm for **4**. Changing the polarity of the solvent lacks any notable impact on the overall absorption spectra (Figure S20).

Acquiring the absorption spectra of the one-electron oxidized form of **4** and of the one-electron reduced form of C_{60} deemed necessary to identify possible charge separation products in the femto- and nanosecond pump-probe experiments – *vide infra*. All measurements were conducted in deaerated anisole with 0.1 M $TBAPF_6$ as supporting electrolyte. Differential absorption spectra of **4** upon one-electron oxidation include maxima at 500 and 750 nm as well as a minimum around 855 nm. One electron reduction of C_{60} results in a weak maximum at 760 nm as well as a strong maximum at 1000 nm along with a shoulder at 1075 nm (Figure S21).

Excited-state characterization of *all-fullerene* 6a/6b

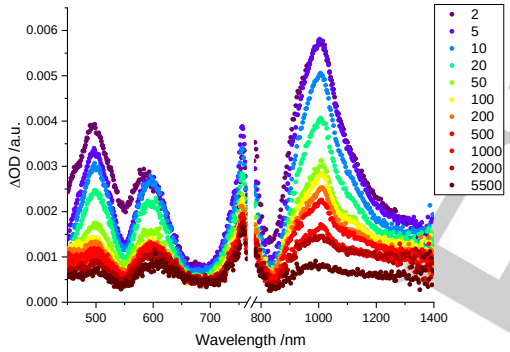

Figure 4. Differential absorption spectra obtained upon femtosecond flash photolysis (387 nm) of **C_{60}-$Lu_3N@I_h$-C_{80}** in deaerated anisole with several time delays between 2 and 5500 ps at room temperature.

The nature of the singlet excited-state deactivation in **6a/6b**, that is, charge separation and charge recombination, was corroborated by means of time-resolved transient absorption spectroscopy. 387 nm was chosen to photoexcite **6a/6b**. In reference experiments with **4** (Figures S22-25), its singlet excited state with its characteristic 495 and 580 nm maxima decay within less than 100 ps to afford the triplet excited state in good agreement with earlier findings on TNTs.[7,17] The latter is characterized by a broad absorption, which maximizes at around 690 nm and a slow reinstatement of the ground state with 1.02 ± 0.01 x 10^6 s^{-1}.

Figure 4 documents the same singlet excited state features upon photoexcitation of **6a/6b**. A fast decay of the singlet excited state starts, however, in **6a/6b** and with 1.83 ± 0.03 x 10^{11} s^{-1} changes in the differential absorption spectra are associated with the transformation into a $C_{60}^{\bullet-}$-$Lu_3N@I_h$-$C_{80}^{\bullet+}$ CS state. In the visible, a newly formed 500 nm maximum matches the fingerprint absorption of the one-electron oxidized form of $Lu_3N@I_h$-C_{80} next to the 750 nm absorption. In the near-infrared, a 1010 nm maximum resembles the marker of the one-electron reduced form of C_{60}. Once formed, the $C_{60}^{\bullet-}$-$Lu_3N@I_h$-$C_{80}^{\bullet+}$ CS state decays biphasic with rate constants of 8.48 ± 0.12 x 10^8 and 1.18 ± 0.01 x 10^8 s^{-1}.

In complementary nanosecond pump-probe experiments, the presence of two $C_{60}^{\bullet-}$-$Lu_3N@I_h$-$C_{80}^{\bullet+}$ CS states were independently corroborated. In addition, the triplet excited state of $Lu_3N@I_h$-C_{80} was verified to be the product of charge recombination. To this end, the broad 690 nm fingerprint absorption as seen in reference experiments with $Lu_3N@I_h$-C_{80} evolves after the charge recombination. It is then the latter, which reinstates slowly the ground state with 1.88 ± 0.01 x 10^6 s^{-1} – a rate constant that fits the decay seen in reference experiments.[18]

Next, deconvolution of the transient spectra into species-associated spectra was performed by means of target analysis. In particular, a kinetic model was employed, which was based on five species. We imply the simultaneous excitation of two different species. On one hand, it is the singlet excited state of $Lu_3N@I_h$-C_{80} with its characteristic 495 and 580 nm maxima as the first species. On the other hand, the CT state is excited and evolves as the second species. Our notion of an excited CT state is confirmed by transient maxima at 500 and 597 nm as opposed to 490 and 577 nm for the singlet excited state of $Lu_3N@I_h$-C_{80}. The CT state decays, however, directly to the ground state with 3.79 ± 0.01 x 10^{10} s^{-1} but without giving rise to any notable charge separation. It is only the singlet excited state, which undergoes charge separation to afford the $C_{60}^{\bullet-}$-$Lu_3N@I_h$-$C_{80}^{\bullet+}$ CS state as the third species. The transient, which evolves throughout the decay of the CS state, still features all the spectroscopic markers of the $C_{60}^{\bullet-}$-$Lu_3N@I_h$-$C_{80}^{\bullet+}$ CS state. As such, we infer that the initially formed CS state is of singlet nature and undergoes a spin flip to yield a triplet CS state as fourth species. Helpful is in this respect the heavy atom affect stemming from the Lu_3N-cluster. The fifth and final species is the triplet excited state of $Lu_3N@I_h$-C_{80}. The aforementioned model and analyses are summarized in Figures 5 and S26-S28.

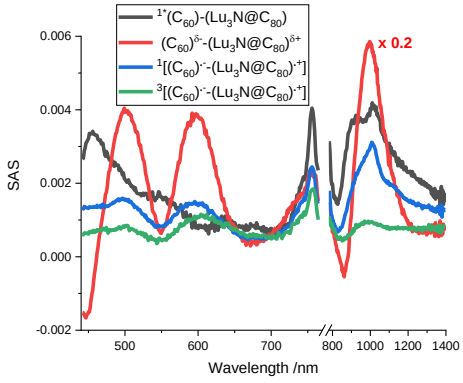

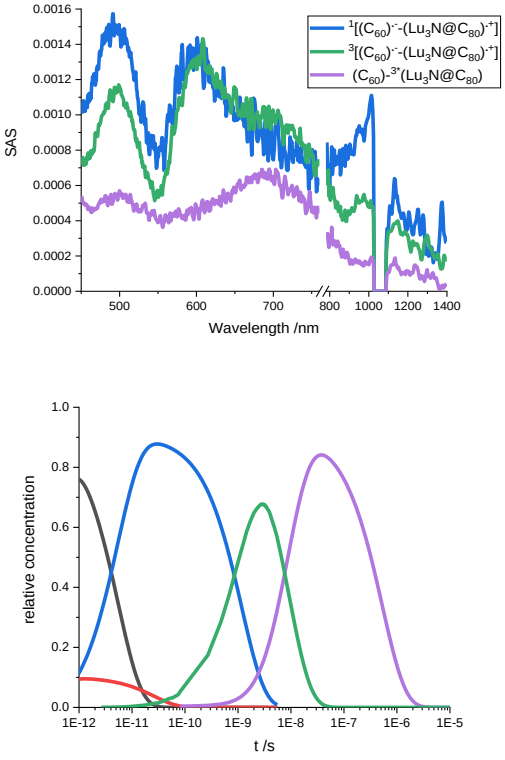

Figure 5. (Top) Species associated spectra of first singlet excited state, CT state, singlet CS state, and triplet CS state obtained upon target analysis of femtosecond transient absorption data of **6a/6b** in anisole. (Center) Evolution associated spectra of singlet CS state, triplet CS state, and triplet excited state of $Lu_3N@C_{80}$ obtained upon global analysis of nanosecond transient absorption data of **6a/6b** in anisole. (Bottom) Corresponding relative concentration profiles of the observed transient species.

In conclusion, we have successfully synthesized and characterized a covalent all-fullerene C_{60}-$Lu_3N@I_h$-C_{80} electron donor-acceptor conjugate. This is, to the best of our knowledge, the first time that fullerenes have been chosen as both electron donors and acceptors in an integrated conjugate. Of great importance is the presence of the Lu_3N cluster, which accelerates spin conversion. Accordingly, combined results from spectroelectrochemical absorption and femtosecond transient experiments support the notion that a $C_{60}^{\bullet-}$-$Lu_3N@I_h$-$C_{80}^{\bullet+}$ charge-separated state is formed. Spin conversion of the singlet $C_{60}^{\bullet-}$-$Lu_3N@I_h$-$C_{80}^{\bullet+}$ charge-separated state into the triplet $C_{60}^{\bullet-}$-$Lu_3N@I_h$-$C_{80}^{\bullet+}$ charge-separated state slows down the charge recombination by one order of magnitude.

Experimental Section

Experimental Details are exhibited in the supporting information.

Acknowledgements

Financial support from the European Research Council (ERC-320441-Chir*all*carbon and the MINECO of Spain (Projects CTQ2017-83531-R, CTQ2017-85341-P, and CTQ2017-84327-P, network CTQ2016-81911-REDT, and Juan de la Cierva formación contracts FJCI-2016-29448 to A.J.S. and FJCI-2017-32757 to O.A.S.) is acknowledged. This work was also funded by the Deutsche Forschungsgemeinschaft (DFG) *via* SFB 953 “Synthetic Carbon Allotropes”, the Catalan DIUE (2017SGR39, XRQTC, and ICREA Academia 2014 Award to M.S.), and the FEDER fund (UNGI10-4E-801).

Keywords: fullerenes · electroactive dyads · photoinduced electron transfer · stereoisomers · excited states

[1] M. R. Wasielewski, *Acc. Chem. Res.* **2009**, *42*, 1910-1921.
[2] Energy Harvesting Materials, D. I. Andrews, Ed., World Scientific Publishing Co., Singapore, 2005.
[3] a) H. Imahori, D. M. Guldi, K. Tamaki, Y. Yoshida, C. Luo, Y. Sakata, S. Fukuzumi, *J. Am. Chem. Soc.* **2001**, *123*, 6617-6628; b) S. Fukuzumi, K. Ohkubo, T. Suenobu, *Acc. Chem. Res.* **2014**, *47*, 1455-1464; c) C. B. KC, G. N. Lim, F. D'Souza, *Angew. Chem. Int. Ed.* **2015**, *54*, 5088-5092; d) L. Moreira, J. Calbo, J. Aragó, B. M. Illescas, I. Nierengarten, B. Delavaux-Nicot, E. Ortí, N. Martín, J.-F. Nierengarten, *J. Am. Chem. Soc.* **2016**, *138*, 15359-15367.
[4] a) N. Martín, L. Sánchez, B. Illescas, I. Pérez, *Chem. Rev.* **1998**, *98*, 2527-2548; b) A. Zieleniewska, F. Lodermeyer, A. Roth, D. M. Guldi, *Chem. Soc. Rev.*, **2018**, *47*, 702-714.
[5] a) J. R. Pinzón, C. M. Cardona, M. Á. Herranz, M. E. Plonska-Brzezinska, A. Palkar, A. J. Athans, N. Martín, A. Rodríguez-Fortea, J. M. Poblet, G. Bottari, T. Torres, S. S. Gayathri, D. M. Guldi, L. Echegoyen, *Chem. Eur. J.* **2009**, *15*, 864-877; b) S. Wolfrum, J. R. Pinzón, A. Molina-Ontoria, A. Gouloumis, N. Martín, L. Echegoyen, D. M. Guldi, *Chem. Commun.* **2011**, *47*, 2270-2272; c) A. Molina-Ontoria, M. Wielopolski, J. Gebhardt, A. Gouloumis, T. Clark, D. M. Guldi, N. Martín, *J. Am. Chem. Soc.* **2011**, *133*, 2370-2373.
[6] Y. Takano, S. Obuchi, N. Mizorogi, R. García, M. Á. Herranz, M. Rudolf, D. M. Guldi, N. Martín, S. Nagase, T. Akasaka, *J. Am. Chem. Soc.* **2012**, *134*, 19401-19408.
[7] L. Feng, M. Rudolf, S. Wolfrum, A. Troeger, Z. Slanina, T. Akasaka, S. Nagase, N. Martín, T. Ameri, C. J. Brabec, D. M. Guldi, *J. Am. Chem. Soc.* **2012**, *134*, 12190-12197.
[8] a) K. Sato, M. Kako, M. Suzuki, N. Mizorogi, T. Tsuchiya, M. M. Olmstead, A. L. Balch, T. Akasaka, S. Nagase, *J. Am. Chem. Soc.* **2012**, *134*, 16033-16039; b) N. Chen, J. R. Pinzón, L. Echegoyen, *ChemPhysChem* **2011**, *12*, 1422-1425; c) M. Rudolf, L. Feng, Z. Slanina, W. Wang, S. Nagase, T. Akasaka, D. M. Guldi, *Nanoscale*, **2016**, *8*, 13257-13262; d) M. Rudolf, S. Wolfrum, D. M. Guldi, L. Feng, T. Tsuchiya, T. Akasaka, L. Echegoyen, *Chem. Eur. J.*, **2012**, *18*, 5136-5148.
[9] D. M. Guldi, *Chem. Commun.* **2000**, 321-327.
[10] a) D. M. Guldi, N. Martín, *J. Mater. Chem.* **2002**, *12*, 1978-1992; b) C. Atienza, N. Martín, M. Wielopolski, N. Haworth, T. Clark, D. M. Guldi, *Chem. Commun.* **2006**, 3202-3204.
[11] a) D. Zhou, H. Tan, C. Luo, L. Gan, C. Huang, J. Pan, M. Lü, Y. Wu, *Tetrahedron Lett.* **1995**, *36*, 9169-9172; b) L. Gan, D. Zhou, C. Luo, H. Tan, C. Huang, M. Lü, J. Pan, Y. Wu, *J. Org. Chem.* **1996**, *61*, 1954-1961; c) X. Lu, X. He, L. Feng, Z. Shi, Z. Gu, *Tetrahedron* **2004**, *60*, 3713-3716.
[12] M. N. Chaur, F. Melin, A. L. Ortiz, L. Echegoyen, *Angew. Chem. Int. Ed.* **2009**, *48*, 7514.

[13] By means of this approach we have identify that $Lu_3N@I_h$-C_{80} / C_{60} interactions in syn-RRSS and syn-RSSS, phenyl / C_{60} interactions, and C_{60} / aliphatic C_8 chain interactions in anti-RSSS impact the relative stabilities. These as well as the characteristics for selected BCPs are shown in Figure S15 and Table S1.

[14] R. A. Marcus, N. Sutin, *Biochim. Biophys. Acta Rev. Bioenerg.* **1985**, *811*, 265-322.

[15] All experiments were performed with both isomers, **6a** and **6b**, without observing any notable differences. Thus, in the following we focus our discussions on **6a**.

[16] M. Maggini, G. Scorrano, M. Prato, *J. Am. Chem. Soc.* **1993**, *115*, 9798-9799.

[17] B. Liu, H. Fang, X. Li, W. Cai, L. Bao, M. Rudolf, F. Plass, L. Fan, X. Lu, D. M. Guldi, *Chem. Eur. J.* **2015**, *21*, 746-752.

[18] No evidence for the involvement of any C_{60} triplet excited state in the overall deactivation cascade was noted (see: D. M. Guldi, M. Prato, *Acc. Chem. Res*., **2000**, 33, 695-703).

Entry for the Table of Contents (Please choose one layout)

Layout 1:

COMMUNICATION

Spin conversion of the singlet charge-separated state into the triplet charge-separated state slows down the charge recombination by one order of magnitude.

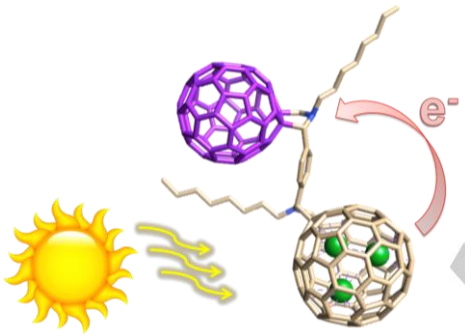

Marta Izquierdo, Benedikt Platzer, Antony, J. Stasyuk, Olga A. Stasyuk, Alexander A. Voityuk, Sergio Cuesta, Miquel Solà, Dirk M. Guldi,* and Nazario Martín**

Page No. – Page No.

***All-fullerene* Electron Donor-Acceptor Conjugates**

Layout 2:

COMMUNICATION

((Insert TOC Graphic here))

*Author(s), Corresponding Author(s)**

Page No. – Page No.

Title

Text for Table of Contents